Figure S1.

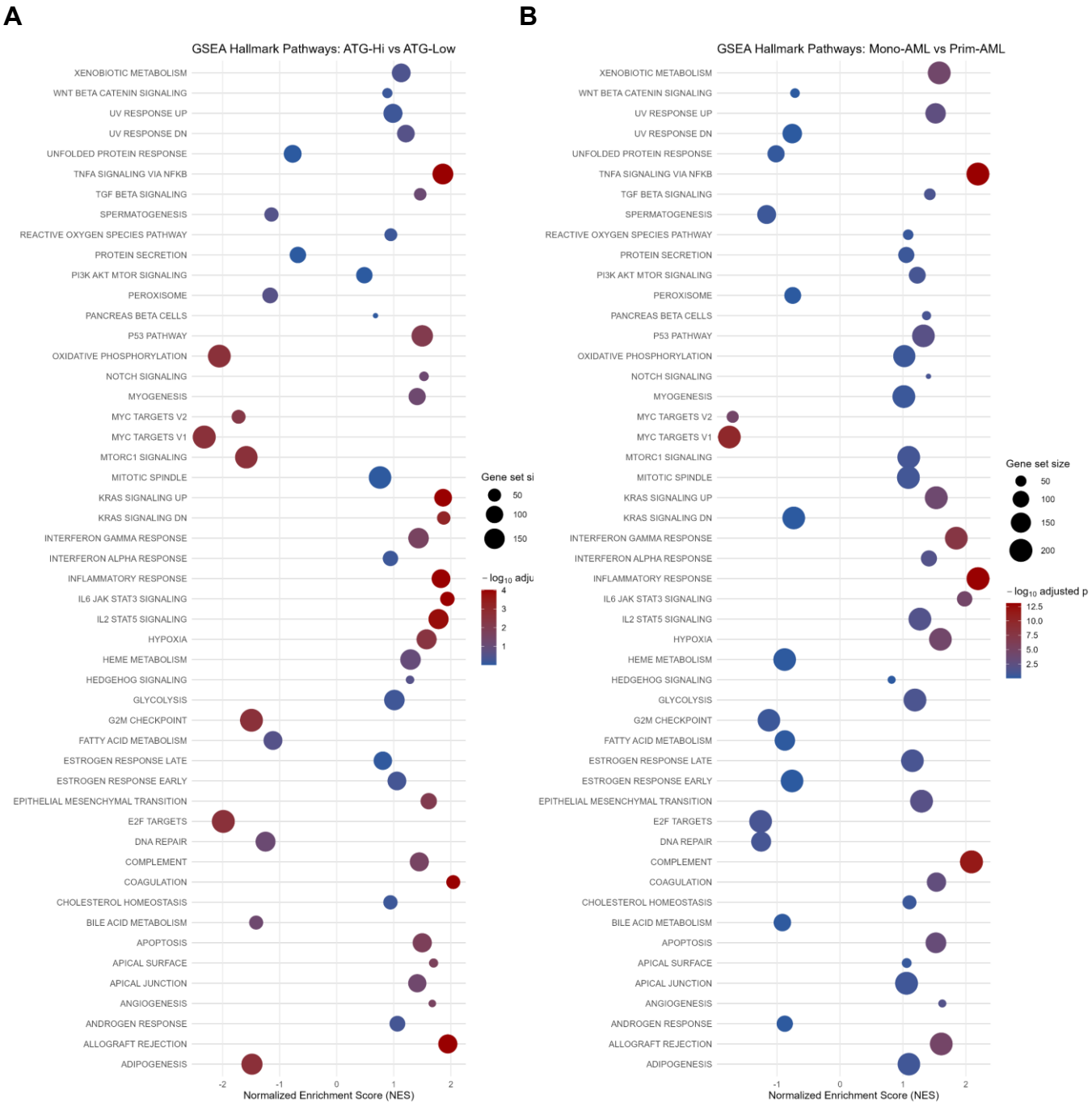

Figure S1. Both stable differentiation-based high autophagy, as seen in monocytic AML subclones, and transient high autophagy is associated with Venetoclax resistance and inflammatory signaling. (A) Hallmark Pathways from GSEA of sorted Molm13 autophagy high (ATG-Hi) vs autophagy low (ATG-Low) RNA-Seq. **(B)** Hallmark Pathways from GSEA of monocytic vs primitive AML LSC RNA-Seq data from Pei et al. 2020.

Figure S1.

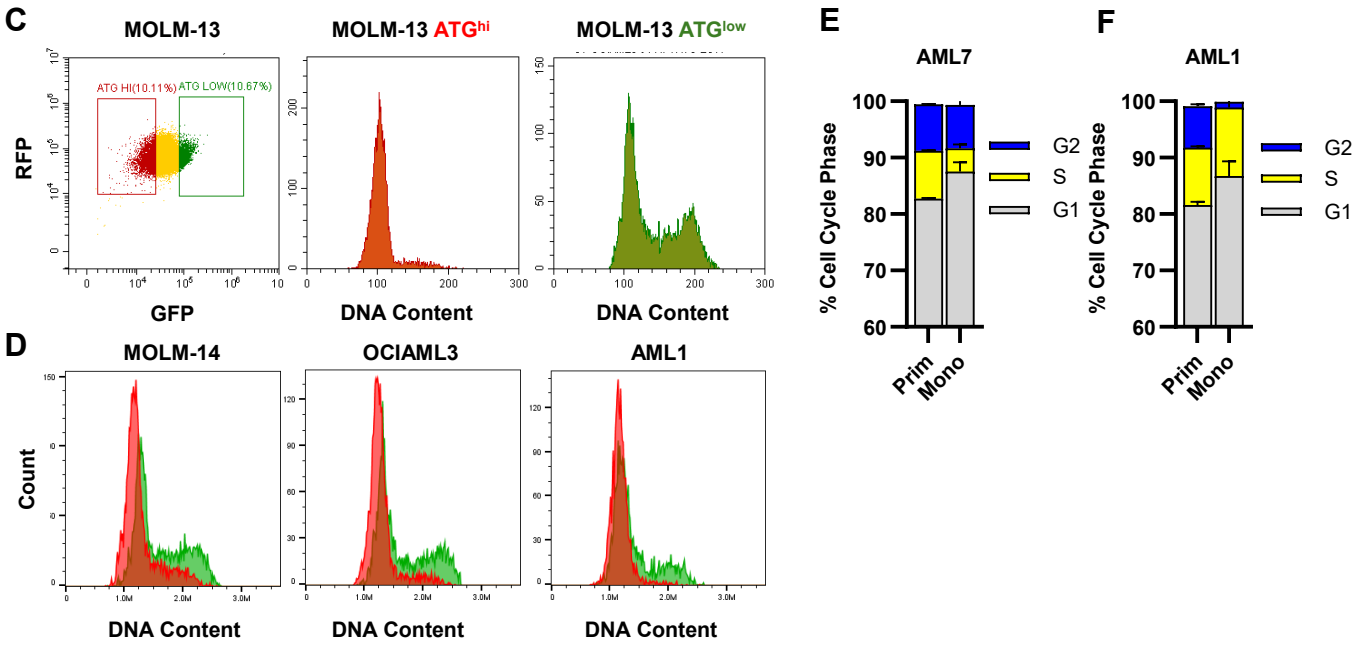

Figure S1. Continued. Transient autophagic flux is in part explained by cell cycle. (C) Cell cycle analysis of Molm13 cells harboring the GFP-LC3-RFP autophagy reporter derived from a single cell clone, stained with Hoechst 33342 to measure DNA content, gated autophagy high cells (high RFP/GFP ratio) are predominantly in G1 of the cell cycle where low autophagy cells are dispersed to all stages of the cell cycle. **(D)** Overlayed cell cycle profiles of autophagy high and low cells for cell lines Molm14, OCIAML3, and primary AML1 harboring the GFP-LC3-RFP autophagy reporter. **(E and F)** Cell cycle profiles of primary AML7 and AML1 gated by primitive (low CD11b and CD14) and monocytic (high CD11b and CD14) subpopulations.

Figure S2.

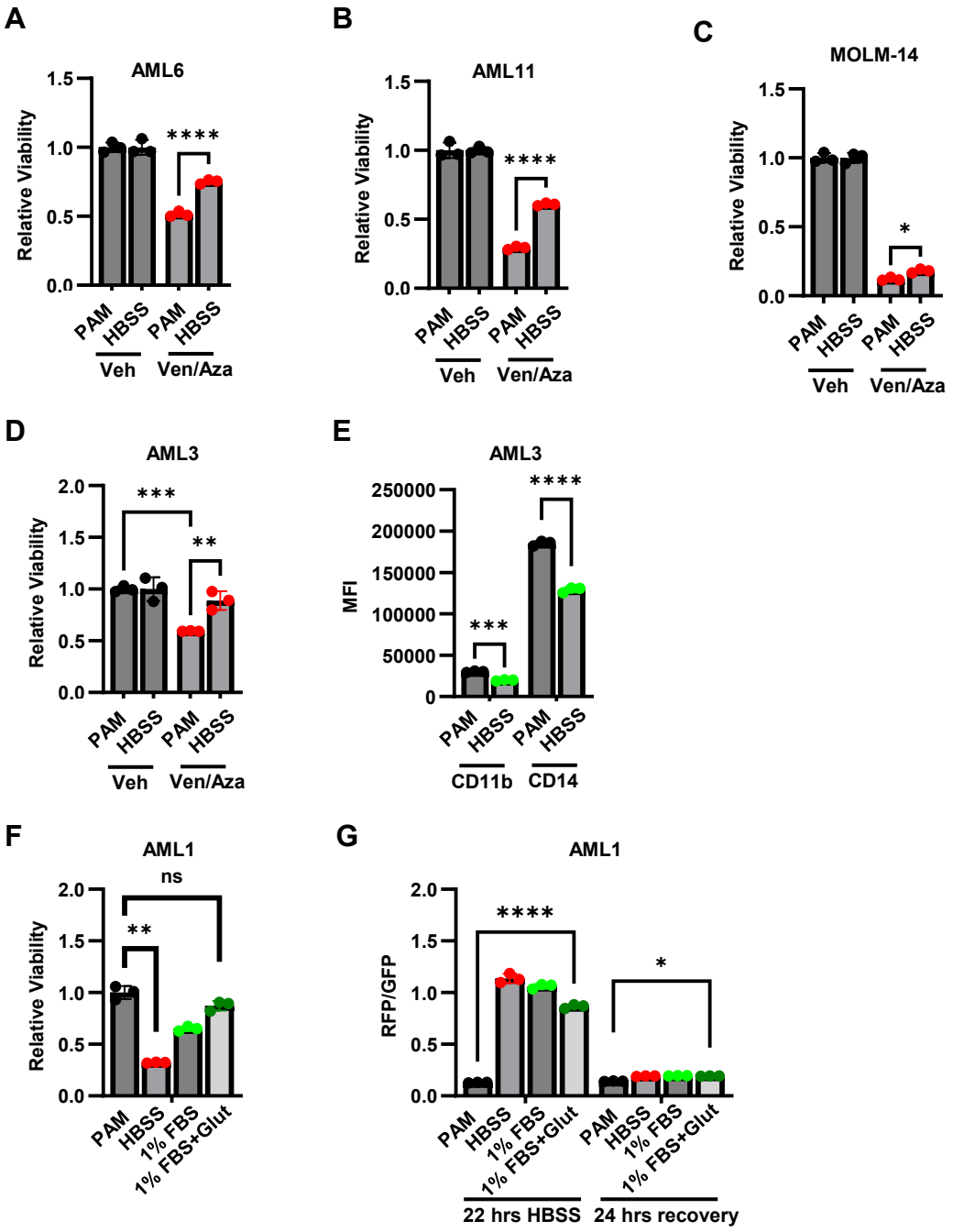

Figure S2. Starvation induced autophagy promotes VenAza resistance. (A, B, C, and D) Relative viability of AML6, AML11, MOLM-14, or AML3 either pretreated in HBSS media for 24hrs (starve) or not, then resuspended into PAM (or RPMI for MOLM-14) and treated with 500nM Venetoclax and 1.5uM Azacitidine for 48hrs. **(E)** MFI of CD11b and CD14 myeloid surface markers of cell in D. **(F)** Relative viability of primary AML1 pretreated in PAM (Ctrl), HBSS, HBSS supplemented with 1% FBS, or HBSS supplemented with 1% FBS and 2mM glutamine for 22 hrs, then resuspended into PAM and allowed to recover for an additional 24hrs. **(G)** Autophagic flux as measured by RFP/GFP ratio of the GFP-LC3-RFP autophagy reporter of cells in H pre and post 24hr recovery in PAM. Error bars represent SEM, two-way ANOVA with Tukey's multiple comparisons test; *, $P < 0.05$; **, $P < 0.01$; ***, $P < 0.001$; and ****, $P < 0.0001$.

Figure S3.

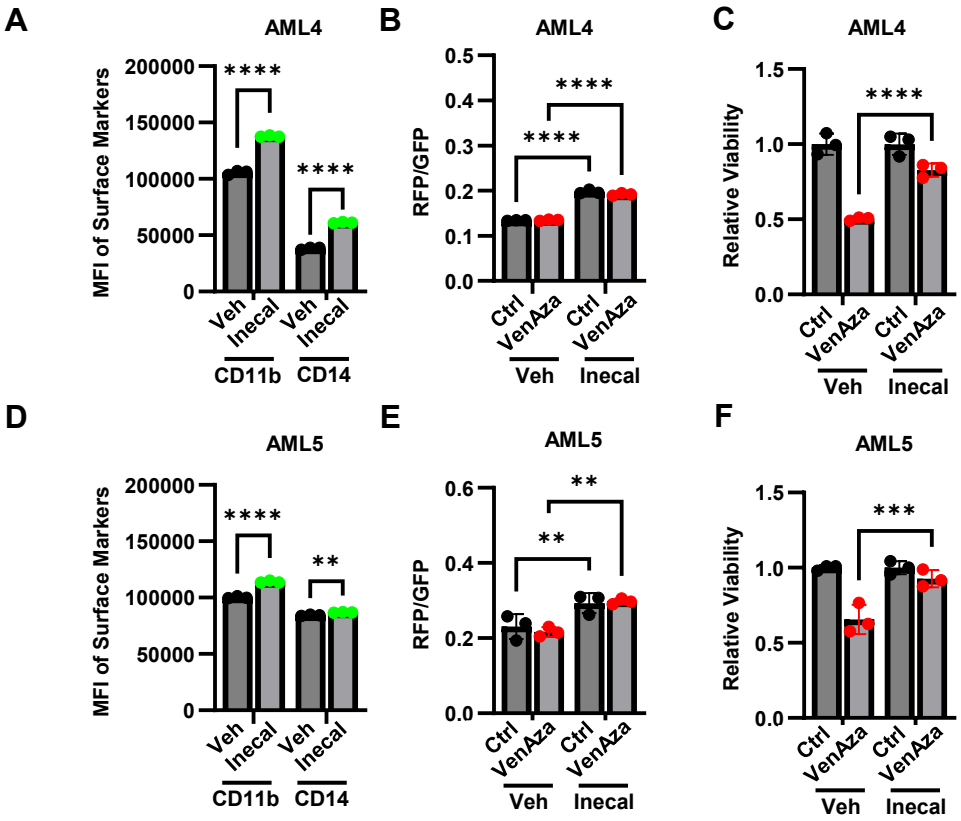

Figure S3. Vitamin D receptor agonist inecalcitol induces AML differentiation, increases autophagic flux and venetoclax resistance. (A and D) MFI of myeloid surface markers CD11b and CD14 of primary AML0801, and AML0805 cells treated with 20nM Inecalcitol for 72 hrs. **(B and E)** MFI of RFP/GFP ratio of AML0801 and AML0805 cells treated with 20nM Inecalcitol for 72 hrs, then treated with 500nM venetoclax and 1.5uM azacitidine for an additional 48 hrs. Error bars represent SEM, two-way ANOVA with Tukey's multiple comparisons test; *, $P < 0.05$; **, $P < 0.01$; ***, $P < 0.001$; and ****, $P < 0.0001$.

Figure S4.

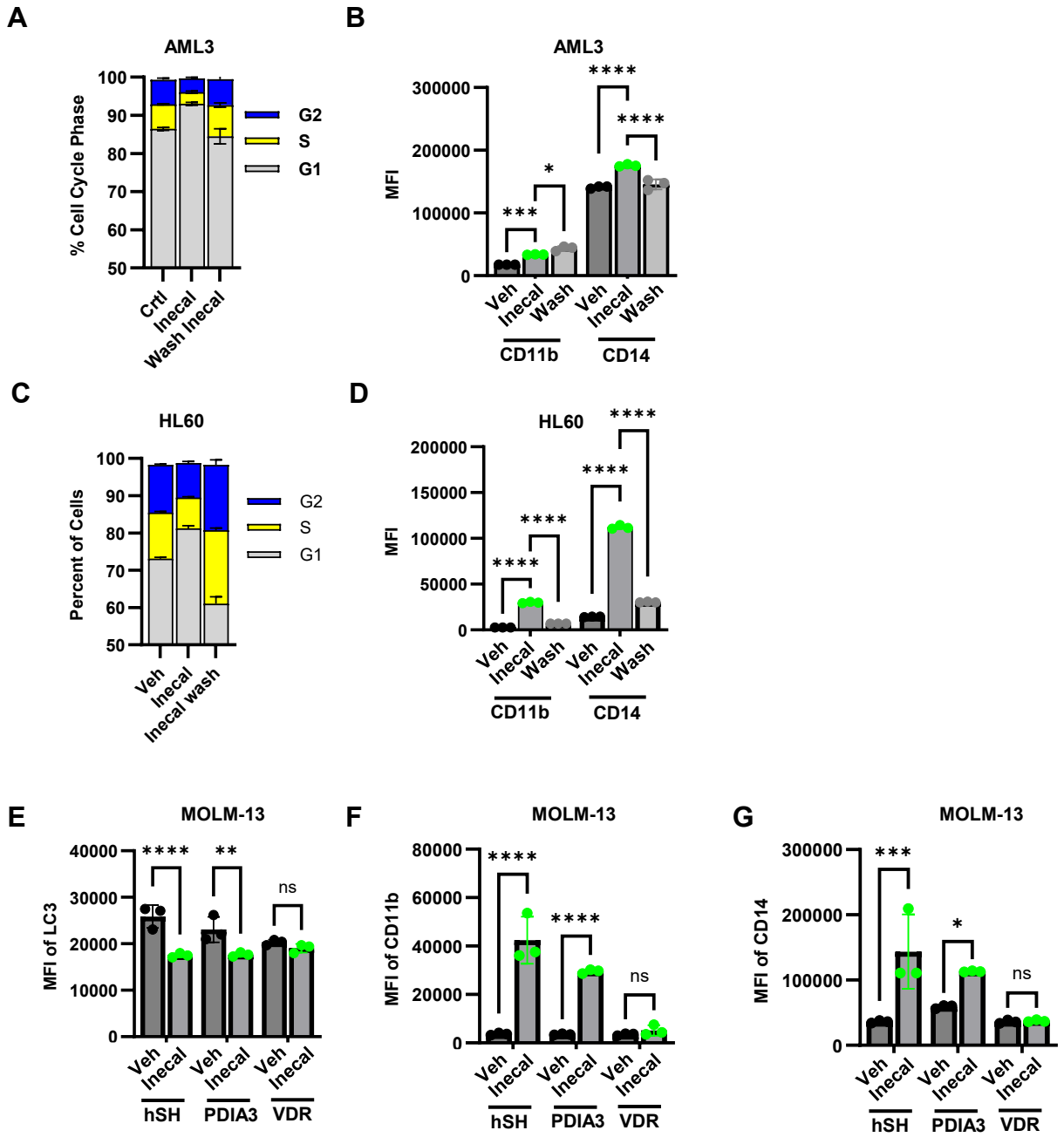

Figure S4. Effects of inecalcitol on autophagic flux, cell cycle, and AML differentiation are reversible and depend on VDR. (A and C) Cell cycle profiles of primary AML3 amd AML cell line HL60 respectively, as measured by Hoechst 33342 staining, treated with 20nM Inecalcitol for 5 days then washed and allowed to recover for an additional 5 days. **(B and D)** MFI of myeloid surface markers CD11b and CD14 of cells in A and C. **(E)** MFI of GFP-LC3 of Molm13 cells treated with 20nM Inecalcitol for 72hrs, harboring Cas9-Blast, the GFP-LC3 autophagy reporter, and LentiGuild-dTOM vectors for CRISPR mediated knockout of either VDR, PDIA3, or hSH (human safe harbor locus). **(F and G)** MFI of myeloid surface markers CD11b and CD14 of cells in E. Error bars represent SEM, two-way ANOVA with Tukey's multiple comparisons test; *, $P < 0.05$; **, $P < 0.01$; ***, $P < 0.001$; and ****, $P < 0.0001$.

Figure S4.

H

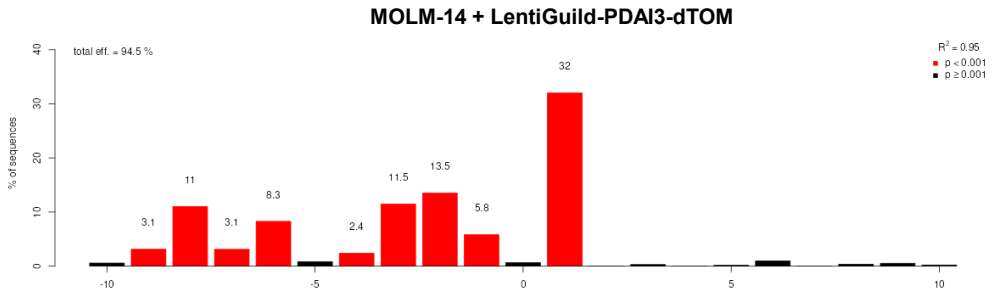

I

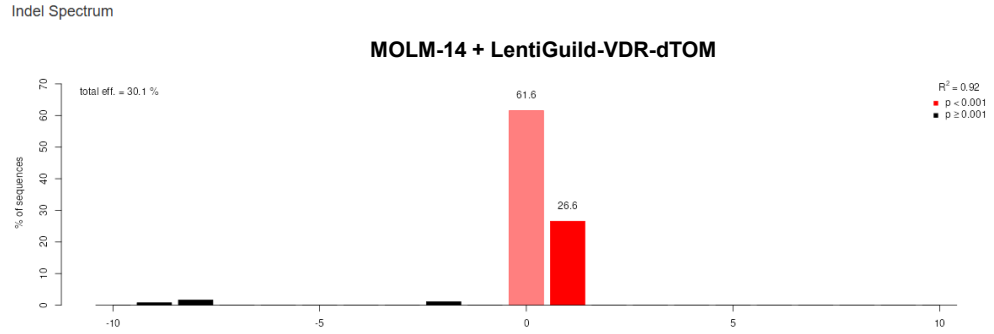

Figure S4 Continued. TIDE analysis of endogenous *VDR* and *PDIA3.* Human cell line MOLM-14 harboring Cas9-Blast and autophagy reporter GFP-LC3 were transduced with LentiGuild-dTOM containing gRNA inserts targeting the human *VDR* or *PDIA3* genes (H) *VDR* targeted in MOLM-14. (I) *PDIA3* targeted in MOLM-14.

Figure S5.

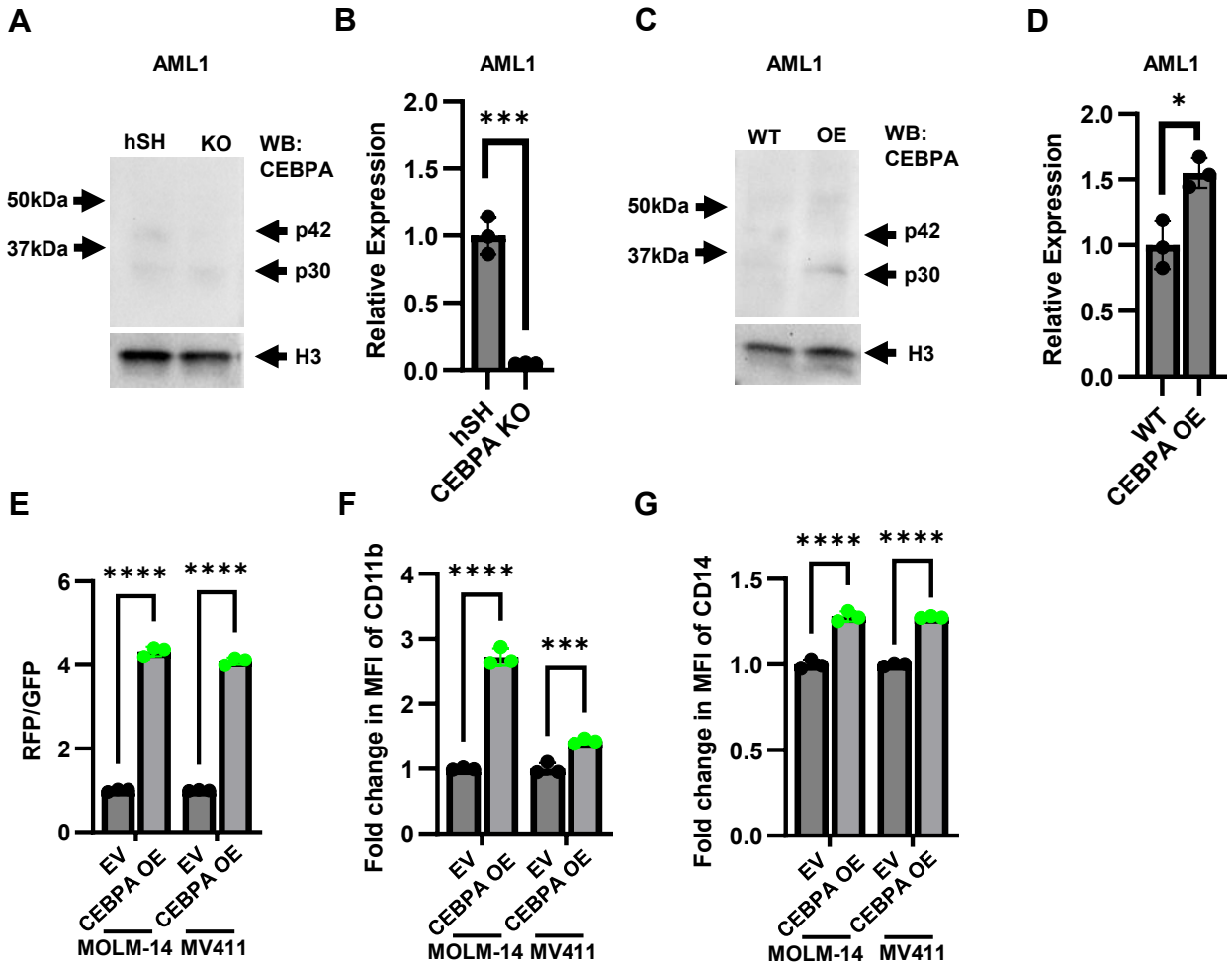

Figure S5. Driver of hematopoietic differentiation CEBPA controls autophagy and Venetoclax resistance. (A) Western blot against CEBPA or histone H3 as loading control, of primary AML1 14 days post transduction with either the human safe harbor (hSH) lentiGuild-mCherry-hSH or lentiGuild-mCherry-CEBPA guild RNA expressing constructs, 2 days post transduction cells were electroporated with 1.5 µg of Cas9 mRNA per 200 000 cells. **(B)** Normalized CT values of qPCR with primers targeting CEBPA of cDNA prepared from cells in A, normalized to bACTIN then WT. **(C)** Western blot of ectopic expression of CEBPA (OE),14 days post transduction of pUltra-CEBPA-GFP. **(D)** Normalized CT values of qPCR with primers targeting CEBPA of cDNA prepared from cells in C, normalized to bACTIN then WT. **(E)** RFP/GFP ratio of Moml14 and MV411 cells 9 days post transduction with pUltra-CEBPA-GFP. **(F)** MFI of CD11b for cells in E. **(G)** MFI of CD14 of cells in E**.** Error bars represent SEM, two-way ANOVA with Tukey's multiple comparisons test; *, P < 0.05; **, P < 0.01; ***, P < 0.001; and ****, P < 0.0001.

Figure S7.

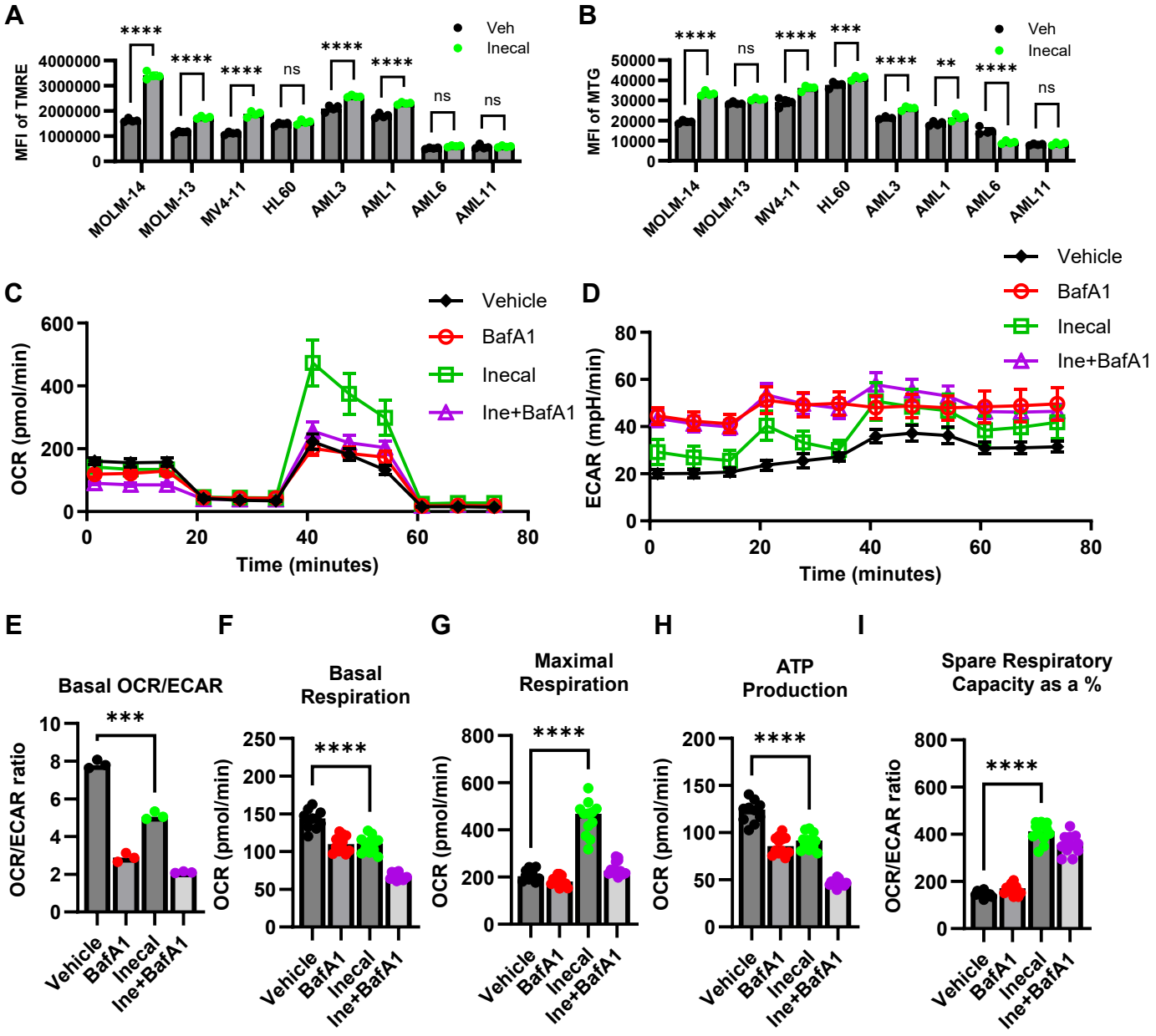

Figure S7. Inecalcitol improves mitochondrial reserve capacity and metabolic flexibility. (A) Mitochondrial transmembrane potential as measured by 30 minutes of TMRE staining of primary AML and cell lines treated with vehicle or 20nM Inecalcitol for 4 days. **(B)** Mitochondrial mass as measured by 30 minutes of MitoTracker staining of cells in A. **(C)** Agilent Seahorse XF Cell Mito Stress Test presenting Oxygen Consumption Rate (OCR) of MV411 treated with 20nM Inecalcitol for 4 days or vehicle, then with or without 100nM Bafilomycin A1 for the last 18hrs just prior to replating cells onto CellTak coated Agilent Seahorse XF Assay plate. Oligomycin, FCCP and Rotenone/AntimycinA treatment at 20, 40 and 60 minutes respectively. **(D)** Extracellular Acidification Rate (ECAR) of cells in C. **(E)** OCR/ECAR ratio at basal time points, pre-oligomycin treatment, of MV411. **(F)** Basal respiration of cell in C. **(G)** Maximal respiration of cell in C. **(H)** ATP production of cell in C. **(I)** Spare respiratory capacity as a precent of cell in C. Error bars represent SEM, two-way ANOVA with Tukey's multiple comparisons test; *, $P < 0.05$; **, $P < 0.01$; ***, $P < 0.001$; and ****, $P < 0.0001$.

MATERIALS AND METHODS (for Supplement)

Vectors and lentiviral production

The GFP-LC3-RFP-expressing vector was generated by cloning the GFP-LC3-RFP sequence from pMRX-IP-GFP-LC3-RFP (Addgene #84573) into the Lentiviral vector pWPXL (Addgene #12257). The *CEBPA*-expressing vector was generated by subcloning the full-length ORF (Sino Biological) into the GFP-expressing Lentiviral vector pUltra (Addgene #24129). The *ATG7* knockdown was achieved via shRNA knockdown with pLKO.1-GFP-shRNA (Addgene #30323). Gene knockouts were achieved via CRISPR using gRNA expressing vectors: lentiGuild-mCherry (Addgene #217005), lentiGuild-Puro (Addgene #52963), or lentiGuild-eGFP (Addgene #99375). See supplemental table for list of cloned in oligo gRNA sequences. Cell lines were transduced lentiCas9-Blast (Addgene #52962) and selected with 10ug/mL Blasticidin S for 1 week prior to lentiGuild vector transduction. Cell lines transduced with lentiGuild-Puro selected with 2ug/mL puromycin for 1 week. Primary AML were electroporated with 1.5 µg of Cas9 mRNA per 200 000 cells with the Neon™ Transfection System 10 µL Kit (ThermoFisher) at 1600 V, 10 ms, 3 pulses, 2 days post transduction with LentiGuild vectors. Cas9 mRNA was transcribed in vitro from SpeI and NheI digested pCas9-PolyA plasmid (Addgene #72602). RNA was purified with the Monarch RNA clean-up kit (NEB) and 5' capped with the ScriptCap™ Cap 1 Capping System (Cellscript), then purified again, resuspended in RNase-free water at 1.8 µg/µL and stored at -80 ºC. Lentiviral particles where produced by transfection of HEK293FT cells with one of the above vectors along with pSPAX2 (Addgene #12260), and pMD2.G (Addgene #12259). HEK293T cells where cultured in DMEM high glucose, pyruvate, supplemented with 10% FBS, 1% Pen/Strep in 10 cm dish at 37 ºC, 5 % CO2 to 50-70% confluence. The medium was changed 2 hours prior to transfection with 15 µM chloroquine added. A transfection mix was prepared by combining the lentiviral plasmids: LentiGuild-gRNA (10 µg/plate), pSPAX2 (10 µg/plate), pMD2.G (6 µg/plate) with PEI Max (at a 1:3 mass ratio) in OptiMEM medium (1 mL per 10 cm plate). The supernatant was harvested after 24hr and 48hrs, filtered and virus was concentrated by ultracentrifugation at 40,000 ×g for 2 h at 4°C over a 20% sucrose cushion. Lentiviral transduction was performed by plating the cells at 500,000–1,000,000/ml with the lentiviral supernatant in the presence of 4 µg/ml polybrene and centrifuging the plate at 1,000 ×g for 1 h at 32°C followed by incubation for 24 h at 37°C, at the end of which the medium was replaced with fresh medium.

Flow cytometry

All flow cytometry experiments were analyzed with a BD CytoFLEX flow cytometer equipped with violet, blue, yellow and red lasers. Cells were washed, resuspended and stained in FACS flow cytometry buffer (PBS without Mg2+ or Ca2+, 2.0% FBS, 2nMM EDTA). For flow cytometric analyses cells were immunostained with fluorophore-linked antibodies (BD Biosciences, eBioscience, Biolegend) against CD11b, CD14 at 1:100 in 50 µL of FACS buffer for 30 minutes, at 4 ºC, in the dark. Cells were washed with 1 mL of FACS buffer, resuspended in 80 µL of FACS buffer + DAPI 100 ng/mL (for live/dead) and analyzed. Data were analyzed using CytExpert Software.

Cell culture

AML cell lines MOLM-13 (RRID:CVCL_2119), MOLM-14 (CVCL_7916), MV4-11(CVCL_0064), HL-60 (CVCL_0002), and OCIAML3 (CVCL_1844) were maintained in IMDM with 2 mM glutamine, 10% heat-inactivated FBS, and 100 U/ml penicillin/streptomycin. Primary AML patient derived samples were generously provided by Dr. Daniel Pollyea (University of Colorado Anschutz Medical Campus, Aurora, CO) and maintained in Primary AML media (PAM): IMDM, 20% BSA, insulin, and transferrin (BIT; Stem Cell Technologies), LDL 1:300 (Millipore Sigma), 50 µM β-mercaptoethanol, 100 U/ml penicillin/streptomycin, 10 ng/ml SCF 10 ng/ml, 10 ng/ml IL-3, and 10 ng/ml FLT3L. All cells were grown at 37 °C in a humidified atmosphere containing 5% CO_2. Characteristics of primary AML samples are tabulated in the Characteristics of patient samples table below.

Cell cycle analysis
Cell cycle analysis was done on live cells to preserve the GFP and RFP signal from the autophagy reporter. Cells were washed with phosphate-buffered saline (PBS) and resuspended in staining buffer containing 10 μg/mL Hoechst 33342 and 100 μg/mL RNase A in PBS and incubated at 4°C in the dark for 30 minutes prior to analysis. Cell cycle distribution was assessed using a BD CytoFLEX flow cytometer. A minimum of 10,000 events per sample were collected, and doublets were excluded based on forward and side scatter properties. Data were analyzed using CytExpert Software and cell populations were gated to quantify the percentage of cells in G0/G1, S, and G2/M phases.

Mitochondrial respiration
Real-time mitochondrial respiration was measured using the Seahorse XFe96 Extracellular Flux Analyzer (Agilent Technologies) and Seahorse XF Cell Mito Stress Test kit as per the manufacturer's instructions. AML cells were treated with the indicated conditions prior to Seahorse assay and plated on Seahorse X96 plates coated with 20 μL/well of Cell-TAK adhesive at 25 μg/mL in 0.1 M $NaHCO_3$ at a concentration of 3×10^5 cells/well suspended in XF base media supplemented with 1 mM pyruvate, 2 mM L-glutamine, 10 mM glucose. OCR measurements were recorded with port injection of oligomycin A (1.5 μM), FCCP (2 μM), and rotenone/antimycin A (0.5 μM) in order. Metrics were calculated as follows. Basal respiration = (Last rate measurement before oligomycin A injection) – (Non-mitochondrial respiration rate); Maximal respiration = (Maximum rate measurement after FCCP injection) – (Non-mitochondrial respiration rate). ATP-linked respiration = (Last rate measurement before oligomycin A injection) - (Last rate measurement before FCCP injection). Spare respiratory capacity = (maximal respiration) – (basal respiration).

Western Blots
Cells were stained with trypan blue and counted using a hemocytometer then lysed in Laemmli buffer (63 mM Tris, 2% sodium dodecyl sulphate, 0.01 % Bromophenol blue, 10% glycerol, pH = 6.8) at 10,000 cell/μL. 20 μL of lysate were loaded on a 4-20% acrylamide gel, then protein were transferred to nitrocellulose membranes, blocked with 5% BSA in TBS-T (150 mM NaCl, 20 mM Tris, 0.1% Tween-20, pH = 7.6), then incubated with antibodies diluted in 1% BSA TBS-T overnight at 4 ºC. Membranes were washed three times with TBS-T, incubated with horseradish peroxidase conjugated secondary antibodies, washed three times with TBS-T, then chemiluminescent substrate was added and the membrane were imaged with a Bio-Rad ChemiDoc MP imager.

RT-qPCR
Total RNA was extracted, purified using RNeasy kit (QIAGEN) and subjected to RT (iScript Reverse Transcriptase supermix, Bio-Rad). Quantitative real-time PCR was performed using a CFX96 PCR system (Bio-Rad), and PCR products were quantified using iTaq Universal SYBR Green Supermix (Bio-Rad).

Statistical analysis
Unpaired Mann-Whitney *U* test or unpaired Student's *t*-test (for bivariate comparison) or two-way ANOVA with Tukey's multiple comparisons test (for multivariate comparison) was performed in Prism software v8 (GraphPad); *, $P < 0.05$; **, $P < 0.01$; ***, $P < 0.001$; and ****, $P < 0.0001$.

GSEA and bubble plots
Gene set enrichment analysis (GSEA) was performed in R using a preranked approach. Genes were ordered by a continuous ranking metric, $\log_2$ fold change, and sorted in decreasing order prior to analysis. Enrichment testing was conducted against the curated gene set MSigDB Hallmark pathways using the fgsea package. Statistical significance was assessed by permutation testing, and p-values were adjusted for multiple testing using the Benjamini–Hochberg false discovery rate (FDR) procedure. For visualization, GSEA results were converted to a tidy data frame and filtered to retain the top enriched pathways based on adjusted p-value and absolute normalized enrichment score (NES). Bubble plots were generated using ggplot2. In these plots, each bubble represents a gene set. The x-axis corresponds to the normalized

enrichment score (NES), and the y-axis lists enriched pathways ordered by NES. Bubble size is proportional to the size of the leading-edge subset (number of genes contributing most to the enrichment score), reflecting the magnitude of pathway involvement. Bubble color encodes statistical significance as the negative $\log_{10}$-transformed adjusted p-value ($-\log_{10}$[FDR]), with higher values indicating stronger enrichment. To ensure numerical stability, adjusted p-values of zero were replaced with the smallest positive representable value prior to log transformation, and missing values were excluded from plotting. All figures were produced using a minimal theme and exported at high resolution for publication.

Key resources table

REAGENT or RESOURCE	SOURCE	IDENTIFIER
Antibodies		
PE-Cy7 Mouse Anti-Human CD14	BD Pharmigen	Cat#557742
APC-Cy7 Rat Anti-CD11b	BD Pharmigen	Cat#557657
PE-Cy7 Mouse anti-human CD11b	BD Pharmigen	Cat# 557743
APC anti-human CD14 Antibody	Biolegend	Cat#325607
Goat Anti-Rabbit IgG (H + L)-HRP Conjugate	Biorad	Cat#1706515
H3	Cell Signaling	Cat#9715
ATG7	Cell Signaling	Cat#2631
CEBPA	Cell Signaling	Cat#2295
Chemicals, peptides, and recombinant proteins		
PEI MAX® - Transfection Grade Linear Polyethylenimine Hydrochloride (MW 40,000)	Polysciences	Cat#25765
Insulin-Transferrin-Selenium-Ethanolamine (ITS -X) (100X)	Gibco	Cat#51500056
DMEN, high glucose, pyruvate	Gibco	Cat#11995065
IMDM	Gibco	Cat#12440053
Penicillin-Streptomycin (10,000 U/mL)	Gibco	Cat#15140122
Fisherbrand™ Research Grade Fetal Bovine Serum, Canadian Sourced	Fischer Scientific	Cat#FB12999102
Sucrose	Millipore Sigma	Cat#S0389-5KG
DAPI	ThermoFisher	Cat#D3571
Hoechst 33342	ThermoFisher	Cat#H3570
Potassium bicarbonate	Millipore Sigma	Cat#237205-500G
O-propargyl puromycin	Vector Labs	Cat#CCT-1407-25
Tetramethylrhodamine, Ethyl Ester, Perchlorate (TMRE)	ThermoFisher	Cat#T669
MitoTracker™ Green FM Dye, for flow cytometry	ThermoFisher	Cat#M46750
Sodium dodecyl sulphate	Millipore Sigma	Cat#L5750
Tween-20	ThermoFisher	Cat#BP330-500
Tris Base	ThermoFisher	Cat#BP152-5
Bromophenol Blue	Fisher Scientific	Cat# AC403151000
Sodium chloride	Fisher Scientific	Cat#S-6713
Immobilon Western Chemiluminescent HRP Substrate	Millipore Sigma	Cat# WBKLS0500
Glycerol	Fisher Scientific	Cat#BP229-1
Cell-TAK	Millipore Sigma	Cat#CLS354240
BIT9500 Serum Substitute	Stem Cell Technologies	Catalog # 09500

Lipoproteins, Low Density, Human Plasma	Millipore Sigma	Cat#437644
human IL-3	Peprotech	Cat#200-03
human SCF	Peprotech	Cat#300-07
human Flt3	Peprotech	Cat#300-19
Critical commercial assays		
T7-FlashScribe™ Transcription Kit	Cellscript	Cat#C-ASF3507
ScriptCap™ Cap 1 Capping System	Cellscript	Cat#C-SCCS1710
iScript™ Reverse Transcription Supermix	Bio-Rad	Cat#1708840
iTaq™ Universal SYBR® Green Supermix	Bio-Rad	Cat#1725124
RNeasy Plus Micro Kit	Qiagen	Cat#74034
Plasmid Plus Maxi Kit	Qiagen	Cat#12943
LIVE/DEAD™ Fixable Near-IR Dead Cell Stain Kit, for 633 or 635 nm excitation	ThermoFisher	Cat#L10119
UltraComp eBeads™ Compensation Beads	ThermoFisher	Cat#01-2222-42
4-20% acrylamide mini protean TGX precast gels	Bio-Rad	Cat#4561095
Phusion™ High-Fidelity DNA Polymerase	NEB	Cat#M0530L
Agilent Seahorse XFe96/XF Pro, Extracellular Flux Assay Kit	Agilant	Cat#103777-100
Agilent Seahorse XFe96/XF Pro, Cell Culture Microplates	Agilant	Cat#103794-100
Seahorse XF Cell Mito Stress Test Kit	Agilant	Cat#103015-100
Seahorse XF Calibrant Solution 500 mL	Agilant	Cat#100840-000
Seahorse XF RPMI assay medium pack, pH 7.4	Agilant	Cat#103681-100
Deposited data		
Aging and *Tet2* KO mouse scRNAseq data	GEO	GSE310533
Experimental models: Cell lines		
HEK293-FT	Cell Technologies Shared Resource (CTSR), Cancer Center, UC Anschutz	CVCL_6911
MOLM-13	CTSR	CVCL_2119
MOLM-14	CTSR	CVCL_7916
MV4-11	CTSR	CVCL_0064
HL-60	CTSR	CVCL_0002
OCIAML3	CTSR	CVCL_1844
THP-1	CTSR	CVCL_0006
U937	CTSR	CVCL_0007
Oligonucleotides		
hSH gRNA: TATTCCCAATGGTACTATGG	IDT (design: this paper)	N/A
hSH-seq-F: AAAATATTGATGCTGTGCCAGA	IDT (design: this paper)	N/A
hSH-seq-R: TGCCTTGTTCCATTTTCACA	IDT (design: this paper)	N/A
hCEPPA gRNA: GTCGGCCGACTTCTACGAGG	IDT (design: this paper)	N/A
hCEPPA-seq2-F: CCAAGAATTCTCCCCTCCTC	IDT (design: this paper)	N/A
hCEPPA-seq2-R: TGGACAAGAACAGCAACGAG	IDT (design: this paper)	N/A
VDR gRNA: GAACGTGCCCCGGATCTGTG	IDT (design: this paper)	N/A
VDR-seq1-F: CCCTTCATGGAAACACCTTG	IDT (design: this paper)	N/A
VDR-seq1-R: AGGGCGAATCATGTATGAGG	IDT (design: this paper)	N/A
PDIA3 gRNA: GGATCCTTACCAGCAGTCCT	IDT (design: this paper)	N/A

PDIA3-seq2-F: CAAGCTCCAGTCTGCCTTTA	IDT (design: this paper)	N/A
PDIA3-seq2-R: TTGTTACCACCAAACTGACCTC	IDT (design: this paper)	N/A
Recombinant DNA		
psPAX2	Addgene	Cat#12260
pMD2.G	Addgene	Cat#12259
pCas9-polyA	Addgene	Cat#72602
pLCv2_U6.(BsmBI).chRNA2_EFS.dTomato_wPRE	Yudovich et al. (dTomato inserted)	
pMRX-IP-GFP-LC3-RFP	Addgene	Cat#84573
pWPXL	Addgene	Cat#12257
pLKO.1 GFP shRNA	Addgene	Cat#30323
pCT GFP LC3	Dr. Gregory	
lentiGuild-mCherry	Addgene	Cat#217005
lentiGuild-Puro	Addgene	Cat#52963
lentiGuild-eGFP	Addgene	Cat#99375
pUltra	Addgene	Cat#24129
lentiCas9-Blast	Addgene	Cat#52962
Software and algorithms	Addgene	Cat#79602
FlowJo™ v11	BD	https://flowjo.com/flowjo/overview
CytExpert Software	Beckman Coulter	https://www.beckman.com/flow-cytometry/research-flow-cytometers/cytoflex/software
GraphPad Prism v10	Dotmatics	https://www.graphpad.com/features
Illustrator	Adobe	https://www.adobe.com/creativecloud/plans.html?plan=edu&product=illustrator
Primer3	Primer3	http://frodo.wi.mit.edu/primer3/
R: A language and environment for statistical computing	R Core Team (2021)	www.R-project.org
ApE: A plasmid Editor	Jorgensen lab	https://jorgensen.biology.utah.edu/wayned/ape/

Supplemental Table 1. Characteristics of patient samples.

AML	Diagnosis	Age	Sex	Karyotyping	Mutations
AML1	Relapse	47	M	46,XY,del(7)(q21)[8]/46,sl,del(5)(q31q35),add(12)(p13)[7]/46,sl,add(12)(p13),del(17)(q21)[3]/46,XY,del(9)(q22q32)[2]	
AML2	DeNovo	60	F	46,XX,t(9;11)(p21;q23)[13]/47,sl,+21[4]/47,sl,+8[3]	KRAS.G13D 23%, KRAS.A146T 6%, PTPN11.T52A 47%
AML3	De Novo			47,XX,+8[15]/47,XX,+11[1]/44-45,XX,add(5)(p12),dic(5;12)(q10;q10),t(11;14)(q13;q32),dic(17;18)(q10;q10), add(20)(q11.2)[cp8]/44,XX,dic(5;12)(q10;q10),der(8)(11qter- > 11q13::14q32- > 14q10::8p11.2- > 8qter),der(11)t(11;14)(q13;q32),dic(17;18)(q10;q10)[2]/46,XX[5]	CBL M400R, SRSF2 P95H, TET2 Q916X and S1290X
AML4	CMML progressed to AML(de novo)	69	M	46,XY,del(7)(q21)[8]/46,sl,del(5)(q31q35),add(12)(p13)[7]/46,sl,add(12)(p13),del(17)(q21)[3]/46,XY,del(9)(q22q32)[2]	IDH1 R132; CKIT D816V
AML5	De Novo	63	M	46,XY[18]	DNMT3A.G550R 40%, DNMT3A.splice site variant 18%, NPM1.W288Cfs*12 22%, ETV6.R103_Y104delinsH 15%, KRAS.G13D 14%, GATA2.R343G 35%
AML6	Relapse	36		Normal karyotype	
AML7	De Novo	62	F	47,XX,psu dic(5;7)(q13;p10),r(7)(p12q11.2),+8,der(12)del(12)(p11.2p13)add(12)(q24.1)[2]/ 44,sl,add(3)(q12),-r(7)(p12q11.2),-8,-der(12)del(12)(p11.2p13)add(12)(q24.1),idic(22)(p11.2), +der(?)(7qter- > 7q11.2::?- > cen- > ?::12q11- > 12qter)[16]/ 45,sdl1,+der(?)(7qter- > 7q11.2::?- > cen- > ?::12q11- > 12qter)[2]	IDH2 R140Q 5%, TP53 L247Q 92% NRAS Q61L 26%
AML8	De Novo therapy-related AML	50	M	46,XY,add(1)(p11),del(5)(q15q33),del(7)(q22q36),der(11)t(1;11)(p31;p12-14)[20]	FLT3-ITD x0.61 38%, BCOR: c.3067T>C p.F1023L 15% NOTCH1: c.7625G>A p.S2542N 12%

AML9	De Novo therapy-related AML	73	M	46,XY[20]	FLT3 p.R595_E596ins28(.58 allelic ratio), NPM1 W288CFs*39%, TET2.L1209P 50%, TET2.H1380D 51%, GATA2.N363delinsKGD 78%
AML10	De Novo	52	M	45,XY,-7[3]/46,sl,+r(7)(p11q21)[11]/46,sdl1,der(5)t(1;5)(q31;p14)[5]/46,XY[1]	ASXL1 c.4120_4121insT; DNMT3A c.885delG; Notch1 c.4746_4747insTGGGGA; NRAS c. 182A>G
AML11				clone 1: +8q, +3q, t(9;22); clone 2: clone 1 abnormalities AND +3, +10, +12 +13, +15 +20; clone 3: clone 2 abnormalities AND der (22); by FISH -7	FLT3-ITD+, WT for NPM1, CEBPA, IDH1 and IDH2